Tetrahedron 73 (2017) 30–38

Contents lists available at ScienceDirect

Tetrahedron

journal homepage: www.elsevier.com/locate/tet

Synthesis and spectroscopic studies of highly fluorescent, solvatochromic diastereomers with differentially stacked bithiophene-substituted quinoxaline rings

Ryan A. Ciufo, John J. Kreinbihl, Sarah R. Johnson, Jocelyn M. Nadeau*

Department of Chemistry, Biochemistry, and Physics, Marist College, 3399 North Road, Poughkeepsie, NY 12601, United States

ARTICLE INFO

Article history:
Received 30 August 2016
Received in revised form
14 November 2016
Accepted 15 November 2016
Available online 17 November 2016

Keywords:
Quinoxaline
Bithiophene
Pi overlap
Intramolecular excimer
Charge transfer
Solvatochromic

ABSTRACT

Diastereomeric C-shaped molecules containing closely stacked bithiophene-substituted quinoxaline rings were synthesized and characterized by NMR, UV–vis absorption, and fluorescence spectroscopy. The unique geometry of each diastereomer resulted in different degrees of π-overlap between the bithiophene-substituted quinoxaline ring chromophores, modulating their spectroscopic properties. The donor-acceptor nature of this chromophore gave rise to its positive solvatochromism. ^{1}H NMR and UV–vis absorption spectroscopy confirmed the existence of π-π interactions in the ground state between the quinoxaline rings in both molecules but between the bithiophene rings only in the *syn* isomer. They exhibited significant emission maxima bathochromic shifts, a strong, positive solvatochromism, increased band broadening, and larger Stokes shifts when compared to a compound with an unstacked chromophore. Additionally, the *syn* isomer consistently showed $\lambda_{max,em}$ value red-shifts and larger band broadening and Stokes shifts compared to the *anti* isomer due to the greater π-overlap in the *syn* isomer.

1. Introduction

It is well established that organic molecules, especially those with π-conjugation, display significant structure-property relationships.[1–4] A better understanding of these relationships is achieved by studying molecules with unique topologies whose molecular properties can be manipulated by synthetic methods. Aromatic molecules are particularly versatile in this regard because they can be synthetically tuned to produce different properties via direct through-bond conjugation[5–10] or through-space interactions between closely stacked aromatic rings.[11–20] Probing the effects of interchromophore interactions between stacked aromatic rings has been the subject of numerous research studies, owing to their importance in a variety of areas of chemistry, most recently as a key design element in molecular electronics applications.[21–28]

We recently reported the synthesis and characterization of diastereomeric C-shaped molecules containing closely, but differently, stacked thiophene-substituted quinoxaline rings (Fig. 1; *anti*- and *syn*-**BT**)[12] that exhibited interesting spectroscopic properties arising, in part, from their unique molecular architecture. Additionally, the donor-acceptor nature of the thiophene-quinoxaline chromophore resulted in their solvatochromism, significantly expanding their emission color range. The different degrees of π-overlap between the chromophores of the diastereomers, where the quinoxaline rings are overlapped in both *anti*- and *syn*-**BT**, but the thiophene rings are overlapped only in *syn*-**BT**, led to their different electronic structures and, in turn, different spectroscopic properties.[19,24,29,30] These results highlight the importance of having well-defined structures in organic electronics applications, as opposed to having a mixture of different molecular orientations in these complex systems, which can have a significant impact on overall device performance.[24,27,31–34] Moreover, using solvent polarity as a means of controlling chromophore emission properties is an important design element because it is easier to change the solvation environment than the structure of a molecule or polymer.[6,35] In this work, we present the results for the next generation of these diastereomeric C-shaped molecules, which contain differentially stacked bithiophene-substituted quinoxaline rings (Fig. 1; *anti*- and *syn*-**BBT**).

Extending each chromophore by an additional thiophene ring was carried out to increase π-conjugation both through-bond and through-space to observe the subsequent impact on their photophysical properties, particularly on their emission spectra.[16] Model compounds **CQT** and **CQBT** were synthesized and studied as

* Corresponding author.
E-mail address: jocelyn.nadeau@marist.edu (J.M. Nadeau).

http://dx.doi.org/10.1016/j.tet.2016.11.044
0040-4020/

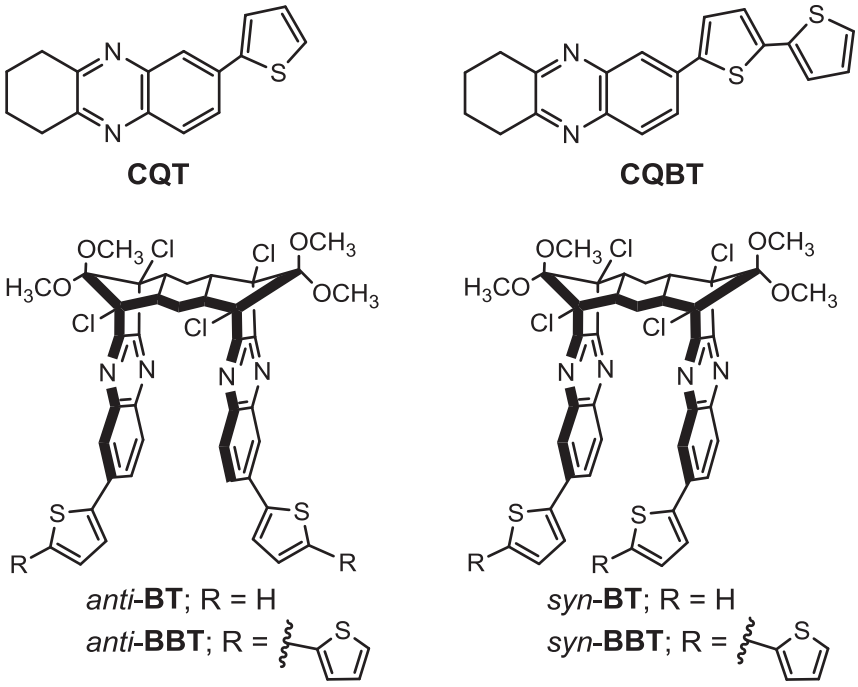

Fig. 1. C-shaped molecules *anti*- and *syn*-**BT** and *anti*- and *syn*-**BBT**; model compounds **CQT** and **CQBT**.

references for understanding the photophysical properties of the lone chromophores in the absence of π-overlap. Herein we present the synthesis and ^{1}H NMR spectroscopy characterization of **CQT**, **CQBT**, *anti*-**BBT**, and *syn*-**BBT** and the results of our analyses of their UV–vis absorption and fluorescence properties as a function of structure and solvent polarity.

2. Results and discussion

2.1. Synthesis and NMR spectroscopy

Diastereomers *anti*- and *syn*-**BBT** were synthesized from their previously reported bromine-substituted precursors (Scheme 1).[12] A microwave-assisted, Pd-catalyzed Suzuki coupling reaction was used to prepare *anti*- and *syn*-**BBT** from *anti*- and *syn*-**BBr**, respectively, and 2,2′-bithiophene-5-boronic acid. *Anti*- and *syn*-**BBT** were purified by chromatography on silica gel, and their isolated yields were 24% and 19%, respectively.

Model compounds **CQT** and **CQBT** were obtained following similar Pd-catalyzed Suzuki coupling procedures with their bromine-substituted precursor, **CQB** (Scheme 2). **CQB** was synthesized by a Zn-catalyzed condensation reaction under microwave-assisted conditions that was previously reported for the synthesis of *anti*- and *syn*-**BBr**.[12]

1,2-Cyclohexanedione was reacted with 1,2-diamino-4-bromobenzene in the presence of a catalytic amount of $Zn(OAc)_2$ to give **CQB** in a 77% yield after chromatography on silica gel. **CQB** was subjected to a microwave-assisted, Pd-catalyzed Suzuki coupling reaction with 2-thienylboronic acid to give **CQT** in 86% yield and with 2,2′-bithiophene-5-boronic acid to give **CQBT** in 69% yield after purification by chromatographic methods. All compounds reported herein were characterized by ^{1}H and ^{13}C NMR spectroscopy and HRMS analysis, with the data fully corroborating the proposed structures.

The NMR spectroscopy data obtained for *anti*- and *syn*-**BBT** were consistent with our previously reported results for *anti*- and *syn*-**BT**,[12] except for the anticipated differences arising from the new thiophene rings. The *syn* isomers have a σ plane of symmetry that cuts in between the aromatic rings through the methylene carbons of the cyclohexane bridging unit, whereas the *anti* isomers have a C_2 axis of symmetry. As observed for *syn*-**BT**, ^{13}C NMR spectroscopy experiments on *syn*-**BBT** illustrate just how similar, yet still chemically different, the two methylene carbons of the central cyclohexane ring are. At 50 MHz, these two carbons appeared as one unresolved peak at 19.9 ppm, but at 100 MHz, there were clearly two peaks at 19.92 and 19.87 ppm (Figure S-5, Supplementary data). The cyclohexane methylene carbons are furthest from the point of difference in these molecules, where the

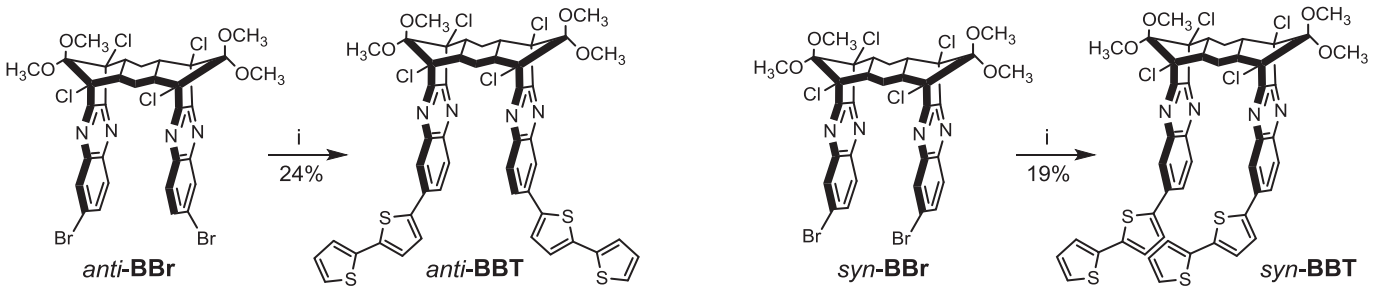

Scheme 1. Synthesis of *anti*- and *syn*-**BBT**. i) 2,2′-bithiophene-5-boronic acid, $Pd(PPh_3)_4$, Na_2CO_3, EtOH, toluene, MW 120 °C, 30 min.

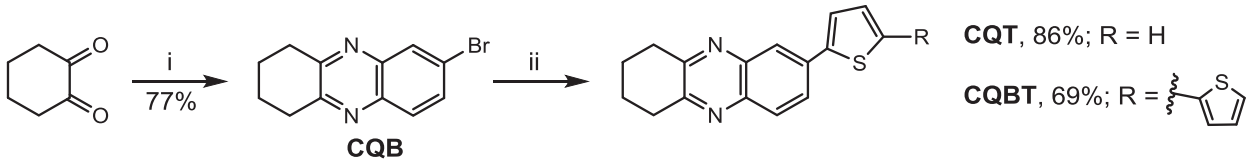

Scheme 2. Synthesis of model compounds **CQT** and **CQBT**. i) 1,2-diamino-4-bromobenzene, $Zn(OAc)_2$, chlorobenzene, MW 200 °C, 30 min; ii) 2-thienylboronic acid (for **CQT**) or 2,2′-bithiophene-5-boronic acid (for **CQBT**), $Pd(PPh_3)_4$, Na_2CO_3, EtOH, toluene, MW 120 °C, 30 min.

thiophene ring attaches to the quinoxaline ring, so they are in chemical environments that are only slightly different. In *anti*-**BBT**, the two cyclohexane methylene carbons are chemically equivalent, resulting in only one peak at 19.9 ppm in its 100 MHz ^{13}C NMR spectrum, as expected (Figure S-4, Supplementary data). Interestingly, the cyclohexane carbons in the model compounds were also difficult to distinguish at 50 MHz. **CQB**, **CQT**, and **CQBT** all lack symmetry, so their carbon atoms are all in different chemical environments. The four cyclohexane carbons should give rise to four aliphatic chemical shifts, specifically two differently shielded pairs where the carbons within each pair are in very similar chemical environments. In the 50 MHz ^{13}C NMR spectrum of **CQB**, there were two unresolved aliphatic chemical shifts at 33.4 and 22.9 ppm. In the 50 MHz ^{13}C NMR spectra of **CQT** and **CQBT**, these same aliphatic carbons were just barely distinguishable at 33.45, 33.39, 23.02, and 23.00 ppm for **CQT** (Figure S-2, Supplementary data) and at 33.46, 33.40, 23.02, and 23.00 ppm for **CQBT**, where the peaks at 23 ppm were just barely separated as a split at the top of the peak. The 100 MHz ^{13}C NMR spectrum of **CQBT** showed two clearly resolved peaks at 33.5 and 33.4 ppm and two nearly resolved peaks at 23.00 and 22.98 ppm (Figure S-3, Supplementary data). As observed for the *syn* isomers of the C-shaped molecules, the chemically nonequivalent cyclohexane carbons at 23 ppm in **CQB**, **CQT**, and **CQBT** were difficult to distinguish because they are furthest from the asymmetric point of attachment of the substituent to the quinoxaline ring.

The aromatic proton chemical shifts in **CQBT**, *anti*-**BBT**, and *syn*-**BBT** were examined to assess the shielding effects and confirm the presence of π-π interactions in the ground state. These interactions were observed in *anti*- and *syn*-**BT**[12] and reported for other molecules with stacked aromatic rings.[15,16,33] Table 1 lists the chemical shift assignments for the aromatic protons of **CQBT**, which represent the shielding environment of these protons in the absence of π overlap, compared to the corresponding proton assignments for *anti*- and *syn*-**BBT**. Protons on the quinoxaline and bithiophene rings of *anti*- and *syn*-**BBT** exhibited the expected upfield shifts to varying degrees due to the shielding effects of the aromatic rings that are directly across from each other, which mirrored the results obtained for *anti*- and *syn*-**BT**.[12] For example, the quinoxaline protons (H_a, H_b, and H_c) in *anti*- and *syn*-**BBT** showed upfield shifts between 0.2 and 0.4 ppm compared to **CQBT**, with H_c in *anti*-**BBT** being shifted upfield by the largest amount compared to all of the protons (0.44 ppm). The thiophene ring protons showed variable degrees of upfield shifts in *anti*- versus *syn*-**BBT** compared to **CQBT**, which was attributed to the bithiophene rings being overlapped in *syn*-**BBT** but not in *anti*-**BBT**. Accordingly, H_d-H_h in *syn*-**BBT** showed consistent upfield shifts compared to the corresponding protons in **CQBT**, especially H_g and H_h (0.32 and 0.37 ppm, respectively). In *anti*-**BBT**, the only thiophene ring proton to show an upfield shift compared to **CQBT** was H_g (0.15 ppm).

These results clearly demonstrate that there are significant π-π interactions in the ground state in *anti*- and *syn*-**BBT** between the aromatic rings that are directly across from one another. The data are easily rationalized upon viewing these structures directly through the aromatic rings (Fig. 2). For the purpose of comparison,

Table 1
Chemical shifts of aromatic protons.

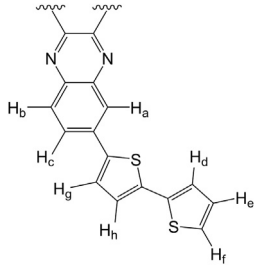

^{1}H Type	Chemical shift (ppm)		
	CQBT	*anti*-**BBT**	*syn*-**BBT**
H_a	8.15	7.92	7.93
H_b	7.94	7.70	7.68–7.74[a]
H_c	7.90	7.46	7.68–7.74[a]
H_d	7.22–7.25[b]	7.27	7.05
H_e	7.04	7.09	6.96
H_f	7.22–7.25[b]	7.31	7.19
H_g	7.39	7.24	7.07
H_h	7.18	7.20	6.81

[a] Multiplet is assigned to both H_b and H_c.
[b] Multiplet is assigned to both H_d and H_f.

the ground-state geometries of *anti*- and *syn*-**BBT** were optimized using density functional theory (DFT) at the B3LYP/6-31G* level of theory.[36] The quinoxaline rings overlap to roughly the same degree in both *anti*- and *syn*-**BBT**, which explains the similar upfield shifts observed for H_a and H_b. The upfield shift observed for H_c was more pronounced for *anti*-**BBT** (0.44 ppm) compared to *syn*-**BBT** (0.16–0.22 ppm), which is consistent with H_c sitting in the shielding zone of the opposite thiophene ring in *anti*-**BBT** but not in *syn*-**BBT**. Accordingly, the only thiophene proton in *anti*-**BBT** that showed an upfield shift compared to **CQBT** was H_g, which is the only thiophene proton in the shielding zone of the opposite

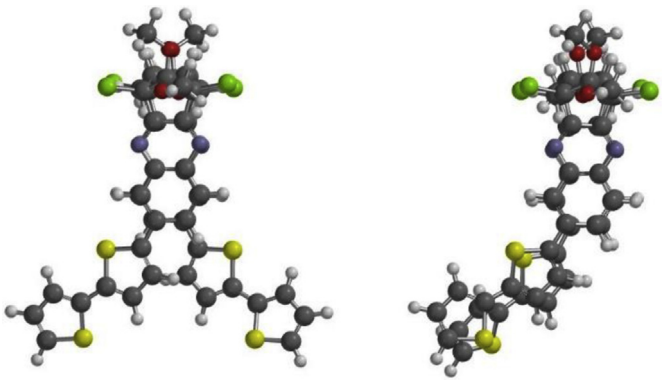

Fig. 2. DFT-optimized (B3LYP/6-31G*) ground-state geometries of *anti*-**BBT** (left) and *syn*-**BBT** (right).

thiophene ring. In *syn*-**BBT**, all the thiophene protons showed upfield shifts compared to the corresponding protons in **CQBT**. Collectively, these results confirm ground-state π-overlap between the quinoxaline rings in both C-shaped molecules and that the bithiophene rings are overlapped in *syn*-**BBT** but not in *anti*-**BBT**.

2.2. UV–vis absorption and fluorescence spectroscopy

Steady-state UV–vis absorption and fluorescence spectroscopy studies were performed on **CQT**, **CQBT**, *anti*-**BBT**, and *syn*-**BBT** in a variety of solvents of increasing polarity from hexanes to methanol (Table 2; Figs. 3 and 4). These experiments were performed to study the impact of the structural differences between these compounds, namely their varying degrees of through-bond and through-space π-delocalization, and solvent polarity on their absorption and emission properties,[37] as compared to those observed for *anti*- and *syn*-**BT**.[12]

Table 2 lists the $\lambda_{max,abs}$ values for each compound in all the solvents studied, and Fig. 3 shows their absorption spectra in representative solvents ranging from nonpolar to polar (hexanes/dichloromethane/methanol). The effect of increasing the through-bond conjugation in going from a thiophene- to a bithiophene-substituted quinoxaline ring can be seen by comparing the absorption spectra of **CQT** to those of **CQBT** (Table 2 and Fig. 3). **CQT**

Table 2
Photophysical properties of **CQT**, **CQBT**, *anti*-**BBT**, and *syn*-**BBT** in solvents of different polarity.

	Solvent	$\lambda_{max,abs}$ (nm)	$\lambda_{max,em}$ (nm)[a]	fwhm (nm)[b]	SS (cm^{-1})[c]	Φ_F[d]
CQT	Hexanes	276, 353	391	54	2753	0.0035
	Cyclohexane	277, 354	390	54	2608	–
	Toluene	357[e]	410	57	3621	0.024
	Ethyl acetate	277, 354	416	60	4210	0.023
	Chloroform	281, 362	428	63	4260	0.13
	Dichloromethane	280, 358	425	64	4404	0.081
	Acetone	354[e]	430	69	4993	0.052
	Acetonitrile	277, 353	431	69	5127	0.083
	n-Butanol	280, 364	454	73	5446	0.53
	Ethanol	280, 365	462	76	5752	0.49
	Methanol	279, 363	467	82	6135	0.56
CQBT	Hexanes	210, 256, 381	417, 440	49	–	0.22
	Cyclohexane	256, 383[e]	419, 444	51	–	–
	Toluene	386[e]	451	65	3734	0.27
	Ethyl acetate	257, 381[e]	463	73	4648	0.12
	Chloroform	259, 390[e]	488	82	5149	0.14
	Dichloromethane	258, 385[e]	485	86	5355	0.15
	Acetone	381[e]	501	97	6287	0.16
	Acetonitrile	211, 257, 379	500	91	6385	0.18
	n-Butanol	206, 259, 390	529	102	6672	0.25
	Ethanol	208, 259, 391	537	111	6953	0.082
	Methanol	208, 259, 388	547	120	7492	0.021
anti-**BBT**	Hexanes	259, 389	434, 457	62	–	0.22
	Cyclohexane	256, 383	436, 461	62	–	–
	Toluene	396[e]	470	73	3976	0.13
	Ethyl acetate	345, 390	499	81	5601	0.16
	Chloroform	349, 401	505	81	5136	0.22
	Dichloromethane	349, 399	517	86	5720	0.35
	Acetone	348, 392	520	94	6279	0.27
	Acetonitrile	347, 397	545	103	6840	0.37
	n-Butanol	348, 398	550	105	6944	0.21
	Ethanol	347, 398	566	113	7458	0.044
	Methanol	347, 398	574	130	7704	0.016
syn-**BBT**	Hexanes	260, 390	463	87	4043	0.058
	Cyclohexane	261, 390	468	84	4274	–
	Toluene	397[e]	499	87	5149	0.12
	Ethyl acetate	342, 390	512	88	6110	0.15
	Chloroform	346, 402	526	89	5864	0.23
	Dichloromethane	347, 400	537	95	6378	0.26
	Acetone	345, 392	534	98	6784	0.21
	Acetonitrile	342, 397	556	106	7203	0.22
	n-Butanol	345, 400	569	110	7425	0.14
	Ethanol	344, 398	579	121	7854	0.044
	Methanol	342, 399	587	147	8027	0.0087

Note: The photographs depict quartz cuvettes containing a solution of each compound in dichloromethane that was being irradiated at 365 nm by a hand-held UV lamp.
[a] λ_{ex} = 350 nm.
[b] fwhm = full width at half maximum.
[c] Stokes shift, SS = $1/\lambda_{max,abs} - 1/\lambda_{max,em}$.
[d] Fluorescence quantum yields were determined relative to coumarin 153 in methanol (Φ_F = 0.45) as the standard (λ_{ex} = 350 nm).[39]
[e] Solvent absorption obscured the short-wavelength analyte absorption.

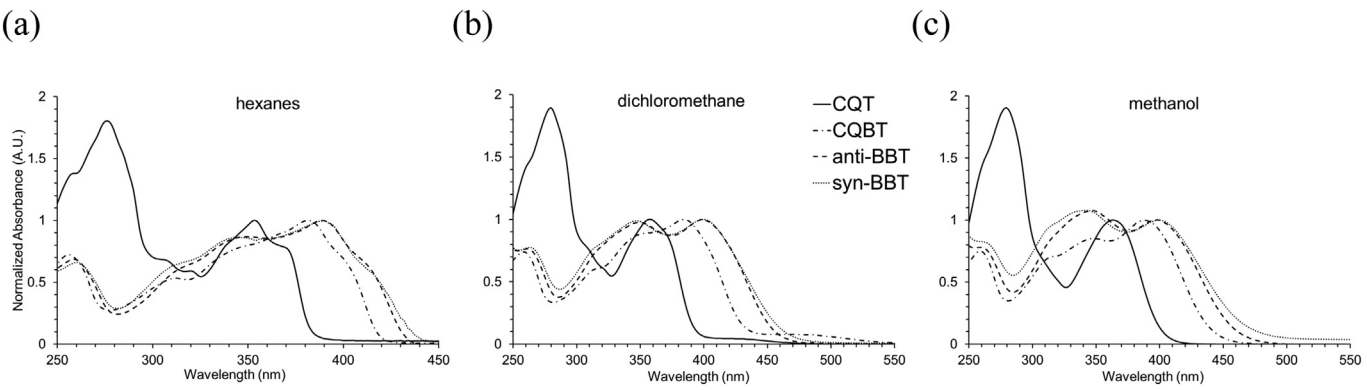

Fig. 3. UV–vis spectra of **CQT** (solid line), **CQBT** (dash-dotted line), *anti*-**BBT** (dashed line), and *syn*-**BBT** (dotted line) in (a) hexanes, (b) dichloromethane, and (c) methanol. The spectra were normalized to the long-wavelength $\lambda_{max,abs}$ value.

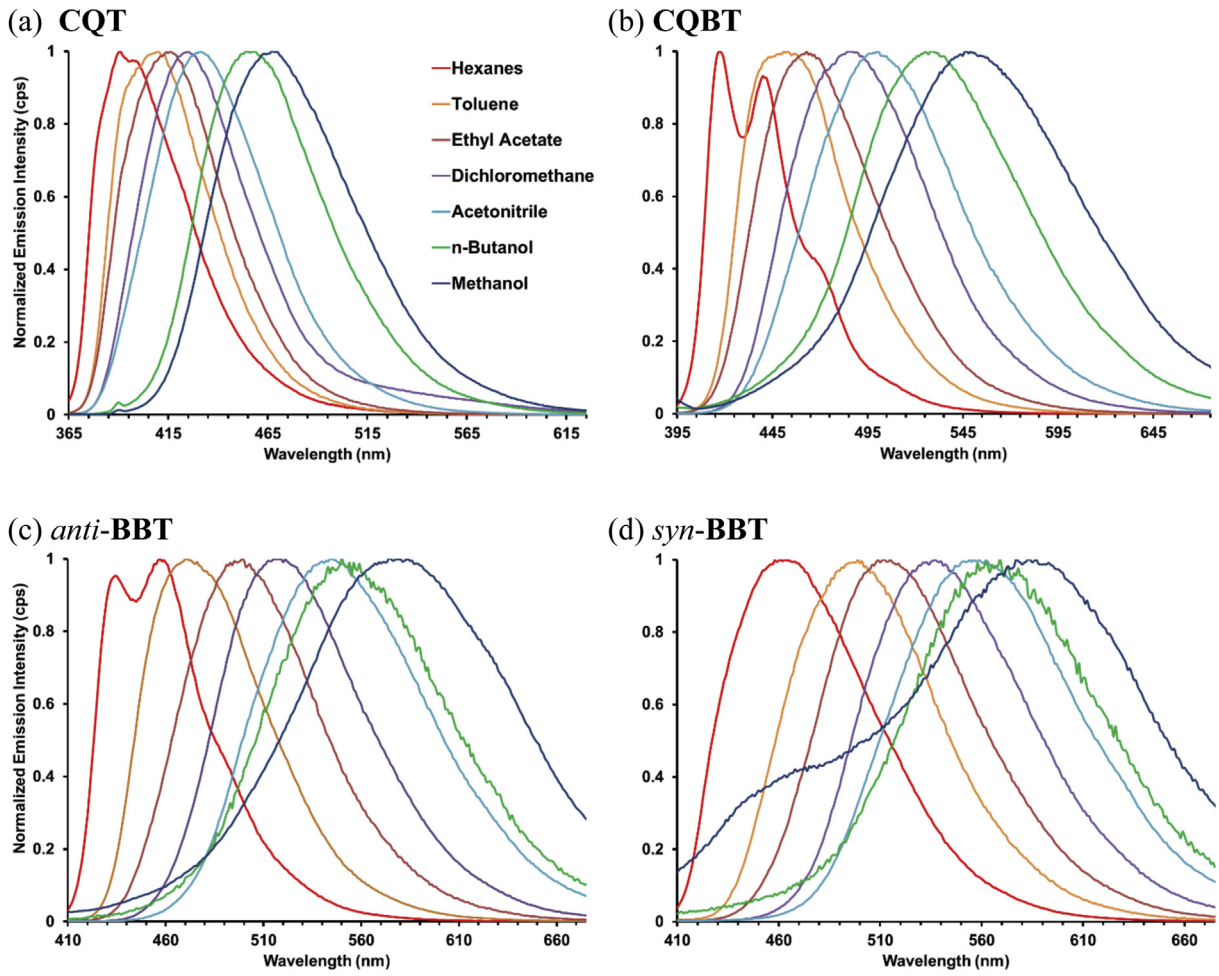

Fig. 4. Fluorescence emission spectra of a) **CQT**, b) **CQBT**, c) *anti*-**BBT**, d) *syn*-**BBT** in various solvents (λ_{ex} = 350 nm). For the sake of clarity, only spectra from representative solvents in the polarity range from Table 2 are presented. The emission intensities are normalized at $\lambda_{max,em}$.

consistently showed two $\lambda_{max,abs}$ bands that appeared in the ranges of 276–281 and 353–365 nm. **CQBT** showed two similar bands, but they look very different and fell within the ranges of 256–259 and 379–391 nm with other vibrational bands in between. **CQBT** also showed a third shorter wavelength $\lambda_{max,abs}$ band between 206 and 211 nm. Within each solvent, the long-wavelength $\lambda_{max,abs}$ band observed for **CQBT** was red-shifted by approximately 30 nm compared to the corresponding band for **CQT**, which is consistent with increased π-conjugation and delocalization in **CQBT** due to the additional thiophene ring.[10,38] The onset of absorption of **CQBT** was significantly red-shifted (>30 nm) compared to **CQT**, which also confirms the increased π-conjugation (Fig. 3). Moreover, comparing the long-wavelength $\lambda_{max,abs}$ band observed for *anti*- and *syn*-**BBT** to the corresponding band observed for *anti*- and *syn*-**BT**[12] also revealed a 30 nm bathochromic shift for the **BBT** derivatives, as expected.

Comparing the UV–vis absorption spectra of **CQBT**, which contains a single, unstacked chromophore, to those of *anti*- and *syn*-**BBT** in any given solvent allows one to analyze the π-stacking effects and their subsequent impact on the electronic properties of the C-shaped molecules (Table 2 and Fig. 3). First, the onset of absorption for *anti*- and *syn*-**BBT** was consistently red-shifted compared those of **CQBT** by 10–20 nm. This result supports the ^{1}H NMR evidence suggesting the presence of π-π interactions in the ground state between the aromatic rings in *anti*- and *syn*-**BBT** that are absent in **CQBT** (*vide supra*).[14,15,30]

Although the absorption spectra and $\lambda_{max,abs}$ values for **CQBT** do not appear to change significantly as a function of solvent polarity, a dramatic change in the absorption spectra can be observed upon examining the data for *anti*- and *syn*-**BBT** from hexanes to methanol (Table 2; Fig. 3). In nonpolar solvents (from hexanes to toluene), the UV–vis spectra of **CQBT**, *anti*-**BBT**, and *syn*-**BBT** were quite similar in overall profile, except for the earlier onset of absorption of the C-shaped molecules that was noted above (for example, see Fig. 3a). As seen in Table 2 for hexanes and cyclohexane, *anti*- and *syn*-**BBT** showed two $\lambda_{max,abs}$ bands (*anti*-**BBT**: 256–259 and 383–389 nm; *syn*-**BBT**: 260–261 and 390 nm) that were similar to those of **CQBT** in all the solvents (256–259 and 379–391 nm). However, in the more polar solvents, the absorption spectra of *anti*- and *syn*-**BBT** changed to a very different profile compared to those of **CQBT**, which did not vary significantly from hexanes to methanol. Specifically, in the polar solvents (from ethyl acetate to methanol), the absorption spectra of *anti*- and *syn*-**BBT** broadened overall and a new blue-shifted $\lambda_{max,abs}$ band appeared at approximately 340 nm that was about equal intensity to or higher than the existing long-wavelength band at approximately 390 nm (*anti*-**BBT**: 345–349 and 390–401 nm; *syn*-**BBT**: 342–347 and 390–402 nm). These results suggest that in nonpolar solvents the electronic transitions available to *anti*- and *syn*-**BBT** are the same as in **CQBT**, namely those of a single bithiophene-substituted quinoxaline chromophore. However, as solvent polarity increases, additional transitions become available to the π-stacked aromatic rings in *anti*- and *syn*-**BBT**.[16] The observed broadening and splitting of the absorption band has been invoked as evidence of electronically interacting chromophores in the ground state.[18,29–31] These findings were consistent with the emission spectroscopy results described below.

The fluorescence emission spectra of **CQT**, **CQBT**, *anti*-**BBT**, and *syn*-**BBT** all showed a broad, structureless, emission band in every solvent studied, except for **CQBT** and *anti*-**BBT** in hexanes and cyclohexane (Table 2 and Fig. 4). Aside from the exceptions noted above that will be discussed shortly, **CQBT**, *anti*-**BBT**, and *syn*-**BBT** demonstrated significant emission maxima bathochromic shifts, a strong, positive solvatochromism, band broadening, and increasing Stokes shifts as solvent polarity increased from hexanes to methanol. To observe the effects of adding the thiophene ring on the emission spectra of the **BBT** family compared to the **BT** family,[12] the difference between the $\lambda_{max,em}$ values of **CQT** and **CQBT** were evaluated in toluene and in methanol. In toluene, there was a 41 nm difference and in methanol, there was an 80 nm difference. The same comparison was made between *anti*-**BT** and *anti*-**BBT** because their thiophene rings do not overlap, so the differences between their $\lambda_{max,em}$ values should also reflect the increased π-conjugation. Accordingly, the difference between their $\lambda_{max,em}$ values in toluene was 43 nm and in methanol was 83 nm, which match the comparison between **CQT** and **CQBT**. The emission spectra of **CQT** were narrower compared to those of **CQBT** in nearly all the solvents studied, where the full-width at half-maximum (fwhm) values observed in toluene to methanol[40] ranged between 57 and 82 nm for **CQT** and between 65 and 120 nm for **CQBT**, respectively. The same trend was observed for the Stokes shifts, which ranged between 3621 and 6135 cm^{-1} for **CQT** and 3734 to 7492 cm^{-1} for **CQBT**. Collectively, these results illustrate the increased through-bond π-conjugation and delocalization in the bithiophene compared to the thiophene analogs, as expected.[10,38] They also suggest that **CQBT** has significantly more excited-state charge-transfer character given its more pronounced solvatochromism and the very large fwhm and Stokes shift values compared to those of **CQT**.[37] Both the thiophene- and bithiophene-substituted quinoxaline rings exhibit donor-accepter characteristics because thiophene and bithiophene are good electron donors and quinoxaline is a good electron acceptor.[41,42] However, given that bithiophene is a better donor than thiophene, the intramolecular charge-transfer (ICT) excited-state character of **CQBT** is expected to be greater than that of **CQT**, as observed.

The $\lambda_{max,em}$ values of **CQBT**, *anti*-**BBT**, and *syn*-**BBT** were examined in solvents ranging in polarity from toluene to methanol to study the effect of the different degrees of π-stacking in the C-shaped molecules.[40] For **CQBT**, the $\lambda_{max,em}$ values were blue-shifted from those of *anti*-**BBT** by an average of 27 nm and from those of *syn*-**BBT** by an average of 44 nm. Additionally, the $\lambda_{max,em}$ values of *syn*-**BBT** were red-shifted by an average of 17 nm compared to those of *anti*-**BBT**. Similar trends were observed within the **BT** family.[12] The dramatic red-shifts observed for the C-shaped molecules compared to the unstacked bithiophene-substituted quinoxaline model, **CQBT**, can be attributed to the overlap between the aromatic rings in *anti*- and *syn*-**BBT** that gives rise to strong, stabilizing π-π interactions in their excited states.[28,30,31] Analogous results have been observed in numerous other molecules that were specifically designed to have closely stacked aromatic rings, where emission in these molecules was said to be from an intramolecular excimer state.[13,14,18,24,29,30,32] It is possible to deconstruct the effects that the different degrees of π-stacking in these molecules have on the emission maxima. The red-shift in the $\lambda_{max,em}$ values for *anti*-**BBT** compared to **CQBT** represents the through-space conjugation of the overlapping quinoxaline rings in *anti*-**BBT** that is absent in **CQBT**. The red-shift in the $\lambda_{max,em}$ values for *syn*-**BBT** compared to *anti*-**BBT** corresponds to the effect of the π-stacked bithiophene rings in *syn*-**BBT** that is absent in *anti*-**BBT**. Finally, the red-shift in the $\lambda_{max,em}$ values for *syn*-**BBT** compared to **CQBT** signifies the effect of the overlapped bithiophene-substituted quinoxaline rings in *syn*-**BBT** that is absent in **CQBT**. Accordingly, the effect of the bithiophene ring overlap (17 nm; 613 cm^{-1}) and the quinoxaline ring overlap (27 nm; 1037 cm^{-1}) numerically adds up to the overall effect of completely overlapping the bithiophene-substituted quinoxaline rings (44 nm; 1650 cm^{-1}). Thus, by comparing and contrasting the $\lambda_{max,em}$ values of **CQBT**, *anti*-**BBT**, and *syn*-**BBT**, it was possible to deconstruct the effects that the different degrees of π-stacking have on their emission maxima. Similar trends were observed for the fwhm and Stokes shift values, which further supports the analysis above.

The emission spectra of **CQBT**, *anti*-**BBT**, and *syn*-**BBT** showed a dramatic dependence on solvent polarity in nearly all the solvents studied (Table 2 and Fig. 4). In hexanes and cyclohexane, the emission spectra of **CQBT** and *anti*-**BBT** exhibited similar, highly structured spectra that both showed two $\lambda_{max,em}$ bands centered around 418 and 442 nm for **CQBT** and 435 and 459 nm for *anti*-**BBT**, in addition to a long-wavelength shoulder. In contrast, the emission spectra of *syn*-**BBT** in hexanes and cyclohexane were broad and structureless with $\lambda_{max,em}$ bands at 463 and 468 nm, respectively. In solvents of increasing polarity from toluene to methanol, the emission spectra of **CQBT**, *anti*-**BBT**, and *syn*-**BBT** were all broad and structureless, and they exhibited a strong, positive solvatochromism. Together, these results suggest that in nonpolar solvents like hexanes and cyclohexane, **CQBT** and *anti*-**BBT** are likely to be emitting from the locally excited (LE) state of the bithiophene-

quinoxaline chromophore. However, in the more polar solvents, the ICT excited-state character of this chromophore is stabilized, and therefore emission in polar solvents is likely to be from an excited state with significant charge-transfer (CT) character.[6,37,43] The fact that all the emission bands of *syn*-**BBT** were broad, structureless, and solvatochromic in all of the solvents studied suggests that the increased through-space π-conjugation from the bithiophene ring overlap, which is absent in **CQBT** and *anti*-**BBT**, stabilizes the excited state, even in nonpolar solvents like hexanes and cyclohexane.[28,30,31]

Furthermore, the fwhm and Stokes shift values for **CQBT**, *anti*-**BBT**, and *syn*-**BBT** were analyzed as a function of solvent polarity, and the results were consistent with the $\lambda_{max,em}$ analysis above. For example, the fwhm values in toluene for **CQBT**, *anti*-**BBT**, and *syn*-**BBT** were 65, 73, and 87 nm, respectively, and the fwhm values in methanol were 120, 130, and 147 nm, respectively. The Stokes shifts also increased as a function of increasing solvent polarity for all three compounds, but the increase was more dramatic for *anti*-**BBT** (toluene to methanol: 3976 to 7704 cm^{-1}) and *syn*-**BBT** (5149 to 8027 cm^{-1}) compared to **CQBT** (3734 to 7492 cm^{-1}) in every solvent, and the increase was greater for *syn*-**BBT** compared to *anti*-**BBT**. These results further corroborate the findings described above, namely, that the bithiophene-substituted quinoxaline ring shows significant CT character in the excited state, which is stabilized by increasing solvent polarity and greater π-overlap.[6,43] The π-overlap between the chromophores in *anti*- and *syn*-**BBT** stabilizes the charge delocalization in the excited state, which leads to broader bands and larger Stokes shifts for the C-shaped molecules compared to **CQBT**.[28,30,31] Moreover, the greater band broadening and larger Stokes shifts observed for *syn*-**BBT** compared to *anti*-**BBT** illustrates the stabilizing effect that the overlapping bithiophene rings have on the excited state of *syn*-**BBT**.

The relative quantum yields of **CQT**, **CQBT**, *anti*-**BBT**, and *syn*-**BBT** measured in a variety of solvents were found to be solvent-dependent, but they did not vary directly with solvent polarity (Table 2).[44] For **CQBT**, *anti*-**BBT**, and *syn*-**BBT**, the quantum yields increased and then decreased with increasing solvent polarity. From toluene to *n*-butanol, the quantum yields for the **BBT** family of compounds fell within a range of 0.12–0.37, but in ethanol and methanol, the values ranged between 0.01 and 0.08. The marked decrease in quantum yield in the polar protic solvents is likely to be due to the emergence of a new, non-radiative deactivation pathway in these hydrogen bond donating solvents.[6,43]

3. Conclusion

In this work, we reported on a new pair of highly fluorescent C-shaped molecules containing differentially stacked bithiophene-substituted quinoxaline rings, *anti*- and *syn*-**BBT**, and related model compounds, **CQT** and **CQBT**, that were synthesized and characterized by NMR, UV–vis absorption, and fluorescence spectroscopy. A detailed analysis of the aromatic ^{1}H NMR chemical shift shielding effects and the UV–vis absorption spectra revealed π-π interactions in the ground state between the quinoxaline rings in *anti*- and *syn*-**BBT**, but π-π interactions between the bithiophene rings only in *syn*-**BBT**. The different degrees of π-stacking in these molecules was also evident from their emission spectra, where *anti*- and *syn*-**BBT** consistently had red-shifted $\lambda_{max,em}$ values and larger band broadening and Stokes shifts compared to **CQBT**, and *syn*-**BBT** consistently showed red-shifted $\lambda_{max,em}$ values, increased band broadening and Stokes shifts compared to *anti*-**BBT**. The C-shaped molecules also showed a remarkably strong, positive solvatochromism that was also observed for **CQBT**, confirming the excited-state ICT character of the bithiophene-substituted quinoxaline ring. Moreover, the increased band broadening and Stokes shifts observed for *anti*- and *syn*-**BBT** compared to **CQBT** as a function of solvent polarity suggested that the through-space π-π interactions between the aromatic rings in the C-shaped molecules stabilize their excited states. Collectively, the **BT**[12] and **BBT** family of C-shaped molecules represent an interesting new class of fluorescent compounds whose emission colors span a wide range across the solvents studied, which suggests that they could be further explored as OLED materials[45] or as solvatochromic polarity probes.[6,35]

4. Experimental section

4.1. General

Microwave-assisted reactions were carried out in a commercially available CEM Discover microwave unit, where the temperature in the reaction vessel was monitored *in situ* using an IR probe. The microwave power was set initially to 200 W and was automatically modulated by the microwave to reach and maintain the target reaction temperature. NMR spectroscopy experiments were conducted on either a 200 MHz or a 400 MHz NMR spectrometer, as specified. Chemical shifts (δ) are reported in parts per million (ppm) and referenced to TMS (δ = 0.00 ppm) for ^{1}H or residual solvent (δ = 77.23 ppm) for ^{13}C. For ^{1}H NMR spectroscopy, peak multiplicities are reported as s, singlet; d, doublet; t, triplet; m, multiplet; and dd, doublet of doublets. Melting points were determined in open capillaries with an electronic apparatus and are uncorrected. $Pd(PPh_3)_4$ was purchased from Strem Chemicals, Inc. All other solvents and reagents were purchased from commercial sources and used without any further purification. Column chromatography was performed using EMD silica gel 60 (230–400 mesh ASTM). TLC and preparative TLC were carried out using EMD TLC silica gel 60 F_{254} plates and on EMD 1 mm silica gel 60 F_{254} plates, respectively. High-resolution mass spectrometry was performed on a QTOF spectrometer. UV–vis absorption and fluorescence spectroscopy measurements were carried out in 1 cm path length quartz cuvettes at room temperature. Relative quantum yields were measured using coumarin 153 in methanol as a reference.[39,44]

4.2. Experimental procedures

4.2.1. 2,9-Diaza-5-bromotricyclo[8.4.0.0^{3,8}]tetradeca-1(10),3,5,7,9-pentaene (*CQB*)

A 10 mL microwave vessel equipped with a stir bar was charged with 50 mg (0.446 mmol) of 1,2-cyclohexanedione, 13 mg (0.071 mmol) of zinc acetate, and 188 mg (1.005 mmol) of 1,2-diamino-4-bromobenzene, followed by 2 mL of chlorobenzene. The headspace was purged with N_2. The vessel was heated to 200 °C for 30 min with stirring in a CEM microwave. The resulting reaction mixture was filtered through a cotton plug, and the solvent was evaporated. The crude product was purified by column chromatography on silica gel (eluent: 20% ethyl acetate in hexanes), and the resulting pink solid was decolorized with activated carbon to give **CQB** as a white solid (90 mg; 77% yield). **CQB** (mp 84.2–85.0 °C): ^{1}H NMR (200 MHz, $CDCl_3$) δ 8.14 (d, J = 2.0 Hz, 1H), 7.83 (d, J = 9 Hz, 1H), 7.39 (dd, J = 8.9, 2.1 Hz, 1H), 3.19–3.10 (m, 4H), 2.08–2.01 (m, 4H); ^{13}C NMR (50 MHz, $CDCl_3$) δ 155.4, 154.8, 142.1, 140.2, 132.6, 131.0, 130.0, 122.8, 33.4, 22.9. HRMS (TOF, ES+): $[M+H]^+$ m/z calcd for $C_{12}H_{12}BrN_2$, 263.0184; found, 263.0184.

4.2.2. 2,9-Diaza-5-(2-thienyl)tricyclo[8.4.0.0^{3,8}]tetradeca-1(10),3,5,7,9-pentaene (*CQT*)

A 10 mL microwave vessel was equipped with a stir bar, 35 mg (0.133 mmol) of **CQB**, 51 mg (0.399 mmol) of 2-thienylboronic acid, 4 mL of toluene, and 1 mL of absolute ethanol. The reaction mixture

was purged with N_2 gas. A 29 mg (0.025 mmol) portion of $Pd(PPh_3)_4$ was added followed by 0.46 mL of a 0.2 g/mL solution of Na_2CO_3. The headspace was purged with N_2 gas. The microwave vessel was heated to 120 °C for 30 min with stirring in a CEM microwave. The reaction mixture was transferred to a separatory funnel and extracted twice with ethyl acetate. The combined organic extracts were washed with water and then brine. The organic layer was dried over anhydrous $MgSO_4$, and the solvent was removed in vacuo. The crude compound was purified by chromatography on silica gel with 30% ethyl acetate in hexanes as the eluent. **CQT** was isolated as an off-white crystalline solid (30 mg; 86% yield). **CQT** (mp 103.9–106.7 °C w/decomp): ^{1}H NMR (200 MHz, $CDCl_3$) δ 8.21–8.19 (m, 1H), 7.96–7.95 (m, 2H), 7.50 (dd, J = 3.6, 1.2 Hz, 1H), 7.37 (dd, J = 5.1, 1.1 Hz, 1H), 7.14 (dd, J = 5.1, 3.7 Hz, 1H), 3.20–3.14 (m, 4H), 2.09–2.02 (m, 4H); ^{13}C NMR (50 MHz, $CDCl_3$) δ 155.0, 154.1, 143.5, 141.7, 140.9, 135.1, 129.0, 128.6, 127.6, 126.3, 124.6, 124.2, 33.45, 33.39, 23.02, 23.00. HRMS (TOF, ES+): $[M+H]^+$ m/z calcd for $C_{16}H_{15}N_2S$, 267.0956; found, 267.0966.

4.2.3. 2,9-Diaza-5-(5-(2′-thienyl)-2-thienyl)tricyclo[8.4.0.0^{3,8}] tetradeca-1(10),3,5,7,9-pentaene (*CQBT*)

A 10 mL microwave vessel equipped with a stir bar was charged with 49 mg (0.186 mmol) of **CQB**, 114 mg (0.543 mmol) of 2,2′-bithiophene-5-boronic acid, 4 mL of toluene, and 1 mL of absolute ethanol. The reaction mixture was purged with N_2 gas. A 0.645 mL portion of an aqueous Na_2CO_3 solution (0.2 g/mL) was added, followed by 41 mg (0.035 mmol) of $Pd(PPh_3)_4$. The headspace was purged with N_2. The vessel was heated to 120 °C for 30 min with stirring in a CEM microwave. Upon completion, the contents were transferred to a separatory funnel, and the biphasic reaction mixture was extracted with ethyl acetate. The combined organic extracts were washed once with water and then with brine. The organic layer was dried over anhydrous $MgSO_4$, and the solvent was removed in vacuo. The crude product was purified by column and preparative chromatography on silica gel (eluent: 30% ethyl acetate in hexanes) to give **CQBT** as a yellow solid (45 mg; 69% yield). **CQBT** (mp 135.2–138.3 °C w/decomp): ^{1}H NMR (400 MHz, $CDCl_3$) δ 8.15 (d, J = 2.0 Hz, 1H), 7.94 (d, J = 8.8 Hz, 1H), 7.90 (dd, J = 8.8, 2.0 Hz, 1H), 7.39 (d, J = 3.6 Hz, 1H), 7.25–7.22 (m, 2H), 7.18 (d, J = 4.0 Hz, 1H), 7.04 (dd, J = 4.8, 3.6 Hz, 1H), 3.16–3.15 (m, 4H), 2.06–2.02 (m, 4H); ^{13}C NMR (100 MHz, $CDCl_3$) δ 155.1, 154.1, 142.0, 141.7, 141.0, 138.3, 137.3, 134.7, 129.1, 128.1, 127.1, 125.3, 125.1, 125.0, 124.2, 123.9, 33.5, 33.4, 23.00, 22.98. HRMS (TOF, ES+): $[M+H]^+$ m/z calcd for $C_{20}H_{17}N_2S_2$, 349.0833; found, 349.0830.

4.2.4. (1α,2β,4β,5α,16α,17β,19β,20α)-7,14,22,29-Tetraaza-1,5,16,20-tetrachloro-31,31,32,32-tetramethoxy-11,26-di(5-(2′-thienyl)-2-thienyl)nonacyclo[18.10.1.1^{5,16}.0^{2,19}.0^{4,17}.0^{6,15}.0^{8,13}.0^{21,30}.0^{23,28}] dotriaconta-6(15),7,9,11,13,21(30),22,24,26,28-decaene (anti-*BBT*)

A 10 mL microwave vessel was equipped with a stir bar, 100 mg (0.120 mmol) of *anti*-**BBr**, 101 mg (0.481 mmol) of 2,2′-bithiophene-5-boronic acid, 4 mL of toluene, and 1 mL of absolute ethanol. The reaction mixture was purged with N_2 gas. A 26 mg (0.022 mmol) portion of $Pd(PPh_3)_4$ was added, followed by 0.415 mL of a 0.2 g/mL solution of Na_2CO_3. The headspace was purged with N_2 gas. The microwave vessel was heated to 120 °C for 30 min with stirring in a CEM microwave. The solution was transferred to a separatory funnel and extracted twice with ethyl acetate. The combined organic extracts were washed once with water followed by another wash with brine. The organic layer was dried over anhydrous $MgSO_4$. The solvent was removed in vacuo. The crude compound was purified by chromatography on silica gel two times with 30% ethyl acetate in hexanes as the eluent. *Anti*-**BBT** was isolated as a yellow solid (29 mg; 24% yield). *Anti*-**BBT** (mp 273 °C w/decomp): ^{1}H NMR (400 MHz, $CDCl_3$) δ 7.92 (d, J = 1.6 Hz, 2H), 7.70 (d, J = 8.8 Hz, 2H), 7.46 (dd, J = 8.6, 2.2 Hz, 2H), 7.31 (dd, J = 5.2, 1.2 Hz, 2H), 7.27 (dd, J = 3.4, 1.0 Hz, 2H), 7.24 (d, J = 4.0 Hz, 2H), 7.20 (d, J = 4.0 Hz, 2H), 7.09 (dd, J = 5.2, 3.6 Hz, 2H), 3.75 (s, 6H), 3.36 (s, 6H), 2.91–2.88 (m, 4H), 2.03–1.98 (m, 2H), –1.05 (m, 2H); ^{13}C NMR (100 MHz, $CDCl_3$) δ 152.7, 151.7, 141.9, 141.2, 140.9, 139.0, 137.3, 135.3, 129.2, 128.3, 127.3, 125.7, 125.2, 125.0, 124.4, 123.7, 111.4, 75.1, 75.0, 52.6, 52.2, 43.5, 43.3, 19.9. HRMS (TOF, ES+): $[M+H]^+$ m/z calcd for $C_{48}H_{37}N_4O_4S_4Cl_4$, 1001.0452; found, 1001.0415.

4.2.5. (1α,2β,4β,5α,16α,17β,19β,20α)-7,14,22,29-Tetraaza-1,5,16,20-tetrachloro-31,31,32,32-tetramethoxy-10,26-di(5-(2′-thienyl)-2-thienyl)[18.10.1.1^{5,16}.0^{2,19}.0^{4,17}.0^{6,15}.0^{8,13}0^{21,30}.0^{23,28}]dotriaconta-6(15),7,9,11,13,21(30),22,24,26,28-decaene (syn-*BBT*)

A 10 mL microwave vessel equipped with a stir bar was charged with 89 mg (0.107 mmol) of *syn*-**BBr**, 135 mg (0.643 mmol) of 2,2′-bithiophene-5-boronic acid, 4 mL of toluene, and 1 mL of absolute ethanol. The reaction mixture was purged with N_2 gas. A 0.37 mL portion of an aqueous Na_2CO_3 solution (0.2 g/mL) was added, followed by 23 mg (0.020 mmol) of $Pd(PPh_3)_4$. The headspace was purged with N_2. The vessel was heated to 120 °C for 30 min with stirring in a CEM microwave. Upon completion, the contents were transferred to a separatory funnel, and the biphasic reaction mixture was extracted with ethyl acetate. The combined organic extracts were washed once with water and once with brine. The organic layer was dried over anhydrous $MgSO_4$, and the solvent was removed in vacuo. The crude product was purified by column chromatography on silica gel with 30% ethyl acetate in hexanes as the eluent. *Syn*-**BBT** was isolated as an orange/yellow solid (20 mg; 19% yield). *Syn*-**BBT** (mp 301–304.5 °C w/decomp): ^{1}H NMR (200 MHz, $CDCl_3$) δ 7.93 (m, 2H), 7.74–7.68 (m, 4H), 7.19 (dd, J = 5.2, 1.2 Hz, 2H), 7.07 (d, J = 4.0 Hz, 2H), 7.05 (dd, J = 3.6, 1.2 Hz, 2H), 6.96 (dd, J = 5.2, 3.6 Hz, 2H), 6.81 (d, J = 3.6 Hz, 2H), 3.74 (s, 6H), 3.35 (s, 6H), 2.93–2.88 (m, 4H), 2.05–1.98 (m, 2H), –1.00 (m, 2H); ^{13}C NMR (100 MHz, $CDCl_3$) δ 152.8, 151.5, 141.9, 140.9, 140.6, 138.5, 137.4, 135.5, 129.3, 128.1, 127.2, 125.5, 124.9, 124.8, 124.0, 123.5, 111.4, 75.10, 75.06, 52.6, 52.2, 43.6, 43.3, 19.92, 19.87. HRMS (TOF, ES+): $[M+H]^+$ m/z calcd for $C_{48}H_{37}N_4O_4S_4Cl_4$, 1001.0452; found, 1001.0433.

Acknowledgements

The authors would like to thank Dr. Karen Walker for her assistance in carrying out the 400 MHz NMR spectroscopy experiments at Vassar College. NMR instrumentation was provided by the US National Science Foundation (NSF-MRI Grant No. 1526982, J. Tanski P.I., T. Garrett co-P.I.). We also thank Laura Wickham for her assistance with compound purification and the Marist College School of Science for financial support.

Appendix A. Supplementary data

Supplementary data related to this article can be found at http://dx.doi.org/10.1016/j.tet.2016.11.044.

References

1. Roncali J. *Macromol Rapid Commun*. 2007;28:1761–1775.
2. Grimsdale AC, Chan KL, Martin RE, Jokisz PG, Holmes AB. *Chem Rev*. 2009;109, 897–1091.
3. Cornil J, Beljonne D, Calbert J-P, Brédas J-L. *Adv Mater*. 2001;13:1053–1067.
4. Murphy AR, Fréchet JMJ. *Chem Rev*. 2007;107:1066–1096.
5. Spitler EL, Monson JM, Haley MM. *J Org Chem*. 2008;73:2211–2223.
6. Gers CF, Nordmann J, Kumru C, Frank W, Müller TJ. *J Org Chem*. 2014;79: 3296–3310.
7. Yao L, Sun S, Xue S, et al. *J Phys Chem C*. 2013;117:14189–14196.
8. Apperloo JJ, Groenendaal LB, Verheyen H, et al. *Chem Eur J*. 2002;8:2384–2396.
9. An Z, Odom SA, Kelley RF, et al. *J Phys Chem A*. 2009;113:5585–5593.

10. Khanasa T, Prachumrak N, Rattanawan R, et al. *J Org Chem*. 2013;78:6702–6713.
11. Chou T-C, Hwa C-L, Lin J-J, Liao K-C, Tseng J-C. *J Org Chem*. 2005;70:9717–9726.
12. DeBlase CR, Finke RT, Porras JA, Tanski JM, Nadeau JM. *J Org Chem*. 2014;79:4312–4321.
13. Chou T-C, Liao K-C, Lin J-J. *Org Lett*. 2005;7:4843–4846.
14. Thirion D, Poriel C, Barrière F, Métivier R, Jeannin O, Rault-Berthelot J. *Org Lett*. 2009;11:4794–4797.
15. Thirion D, Poriel C, Métivier R, Rault-Berthelot J, Barrière F, Jeannin O. *Chem Eur J*. 2011;17:10272–10287.
16. Leung M-k, Viswanath MB, Chou P-T, Pu S-C, Lin H-C, Jin B-Y. *J Org Chem*. 2005;70:3560–3568.
17. Pognon G, Boudon C, Schenk KJ, Bonin M, Bach B, Weiss J. *J Am Chem Soc*. 2006;128:3488–3489.
18. Alamiry MAH, Benniston AC, Copley G, Harriman A, Howgego D. *J Phys Chem A*. 2011;115:12111–12119.
19. Giaimo JM, Lockard JV, Sinks LE, Scott AM, Wilson TM, Wasielewski MR. *J Phys Chem A*. 2008;112:2322–2330.
20. Knoblock KM, Silvestri CJ, Collard DM. *J Am Chem Soc*. 2006;128:13680–13681.
21. Brédas J-L, Beljonne D, Coropceanu V, Cornil J. *Chem Rev*. 2004;104:4971–5003.
22. Riley KE, Hobza P. *Acc Chem Res*. 2013;46:927–936.
23. Schneebeli ST, Kamenetska M, Cheng Z, et al. *J Am Chem Soc*. 2011;133:2136–2139.
24. Jagtap SP, Mukhopadhyay S, Coropceanu V, Brizius GL, Brédas J-L, Collard DM. *J Am Chem Soc*. 2012;134:7176–7185.
25. Hartnett PE, Margulies EA, Matte HSSR, Hersam MC, Marks TJ, Wasielewski MR. *Chem Mater*. 2016;28:3928–3936.
26. Thirion D, Romain M, Rault-Berthelot J, Poriel C. *J Mater. Chem*. 2012;22:7149–7157.
27. Yoo H, Yang J, Yousef A, Wasielewski MR, Kim D. *J Am Chem Soc*. 2010;132:3939–3944.
28. Jagtap SP, Collard DM. *J Am Chem Soc*. 2010;132:12208–12209.
29. Ohkita H, Ito S, Yamamoto M, Tohda Y, Tani K. *J Phys Chem A*. 2002;106:2140–2145.
30. Benten H, Ohkita H, Ito S, et al. *J Phys Chem B*. 2005;109:19681–19687.
31. Bartholomew GP, Bazan GC. *Acc Chem Res*. 2001;34:30–39.
32. Morisaki Y, Sawamura T, Murakami T, Chujo Y. *Org Lett*. 2010;12:3188–3191.
33. Rathore R, Abdelwahed SH, Guzei IA. *J Am Chem Soc*. 2003;125:8712–8713.
34. Garnier F. *Acc Chem Res*. 1999;32:209–215.
35. Reichardt C. *Chem Rev*. 1994;94:2319–2358.
36. Calculated using Spartan '16 for Windows (Version 1.1.0) by Wavefunction, Inc.
37. Reichardt C, Welton T. *Solvents and Solvent Effects in Organic Chemistry*. fourth ed. Weinheim: Wiley-VCH; 2011.
38. Lee SA, Hotta S, Nakanishi F. *J Phys Chem A*. 2000;104:1827–1833.
39. Boens N, Qin W, Basarić N, et al. *Anal Chem*. 2007;79:2137–2149.
40. The analysis was limited to solvents in which only a single, broad emission band was observed.
41. Yamamoto T, Zhou Z-h, Kanbara T, et al. *J Am Chem Soc*. 1996;118:10389–10399.
42. Choi Y-S, Lee W-h, Kim J-R, et al. *Bull Korean Chem Soc*. 2011;32:417–423.
43. Lakowicz JR. *Principles of Fluorescence Spectroscopy*. third ed. New York: Springer; 2006.
44. Fery-Forgues S, Lavabre D. *J Chem Educ*. 1999;76:1260–1264.
45. Zhu X-H, Peng J, Cao Y, Roncali J. *Chem Soc Rev*. 2011;40:3509–3524.